REPORT DOCUMENTATION PAGE

Form Approved
OMB No. 0704-0188

PLEASE DO NOT RETURN YOUR FORM TO THE ABOVE ADDRESS.

1. REPORT DATE *(DD-MM-YYYY)*	2. REPORT TYPE	3. DATES COVERED *(From - To)*
01062004	Journal Article	

4. TITLE AND SUBTITLE

Structural response in steady-state flow of a multi-component driven system: interacting lattice gas simulation

5a. CONTRACT NUMBER

5b. GRANT NUMBER

5c. PROGRAM ELEMENT NUMBER

0601153N

6. AUTHOR(S)
R.B. Pandey, J.F. Gettrust

5d. PROJECT NUMBER

5e. TASK NUMBER

5f. WORK UNIT NUMBER

7. PERFORMING ORGANIZATION NAME(S) AND ADDRESS(ES)
Naval Research Laboratory
Marine Geosciences Division
Stennis Space Center MS 39529

8. PERFORMING ORGANIZATION REPORT NUMBER
NRL/JA/7430-04-7

9. SPONSORING/MONITORING AGENCY NAME(S) AND ADDRESS(ES)

Naval Oceanographic Office
Stennis Space Center, MS 39529

10. SPONSOR/MONITOR'S ACRONYM(S)
NAVO

11. SPONSOR/MONITOR'S REPORT NUMBER(S)

12. DISTRIBUTION/AVAILABILITY STATEMENT

Approved for public release, distribution is unlimited

13. SUPPLEMENTARY NOTES

Physica A 345 (2005) 555-564

14. ABSTRACT

The effects of molecular weights (MA,MB) on the self-organized segregation of immiscible constituents (A,B) driven by pressure bias (H = 0.0-1.0) generated by geologic processes are examined by an interacting lattice gas Monte Carlo simulation. Constituents (A,B), released from a source at the bottom according to their lattice concentrations, can escape the lattice from top or bottom. The longitudinal steady-state density profiles (A,B) depend on their molecular weight and bias with linear, exponential, and non-monotonic decays with the height.

15. SUBJECT TERMS

Self-organized-patterns; Multi-component: Driven system: Interacting lattice gas

16. SECURITY CLASSIFICATION OF:			17. LIMITATION OF ABSTRACT	18. NUMBER OF PAGES	19a. NAME OF RESPONSIBLE PERSON
a. REPORT	b. ABSTRACT	c. THIS PAGE			Ras Pandey
Unclassified	Unclassified	Unclassified	SAR	10	19b. TELEPHONE NUMBER *(Include area code)* 228-688-5480

Available online at www.sciencedirect.com
SCIENCE DIRECT®
PHYSICA A
ELSEVIER
Physica A 345 (2005) 555–564
www.elsevier.com/locate/physa

Structural response in steady-state flow of a multi-component driven system: interacting lattice gas simulation

R.B. Pandey[a,b,*], J.F. Gettrust[a]

[a]*Naval Research Laboratory, Stennis Space Center, MS 39529, USA*
[b]*Department of Physics and Astronomy, University of Southern Mississippi, Hattiesburg, MS 39406-5046, USA*

Received 5 January 2004; received in revised form 1 June 2004
Available online 21 August 2004

Abstract

The effects of molecular weights (M_A, M_B) on the self-organized segregation of immiscible constituents (A, B) driven by pressure bias ($H = 0.0$–1.0) generated by geologic processes are examined by an interacting lattice gas Monte Carlo simulation. Constituents (A, B), released from a source at the bottom according to their lattice concentrations, can escape the lattice from top or bottom. The longitudinal steady-state density profiles (A, B) depend on their molecular weight and bias with linear, exponential, and non-monotonic decays with the height. The transverse density profiles show signatures of partial layering. The total number (N) of constituents remains nearly constant in steady state and seems to decay with the bias, $N \propto H^{-0.14}$ for all but extreme range of H. At $M_A = 0.1$, $M_B \geqslant 0.8$, number of constituents (N_A, N_B) show non-monotonic dependence on H with $N_B \gg N_A$ but a maximum in N_A and minimum in N_B.

PACS: 47.70.M; 61.43.Bn; 64.75; 83.10.Rs; 87.17.Aa

Keywords: Self-organized-patterns; Multi-component; Driven system; Interacting lattice gas

*Corresponding author. Department of Physics and Astronomy, University of Southern Mississippi, Hattiesburg, MS 39406-5046, USA. Tel.: +1-601-266-4485; fax: +1-601-266-5149.
E-mail address: ras.pandey@usm.edu (R.B. Pandey).

0378-4371/$ - see front matter © 2004 Elsevier B.V. All rights reserved.
doi:10.1016/j.physa.2004.07.044

1. Introduction

Flow of fluid mixtures from a reservoir source driven by the fluid pressure bias resulting from compaction of sediments, tectonic processes, geothermal anomalies, etc. is a common natural phenomena in geomarine systems [1–3]. Some examples include dewatering of fine-grained sediments due to overburden pressure, dissociation of methane and hydrocarbon below the ocean floor [4,5], mud volcanoes, free-methane and water, dispersion of complex fluid mixtures consisting of hazardous waste, etc. Understanding the distribution of components would be valuable, particularly when the constituents are dissimilar with different molecular weights as many of these systems. A variety of patterns [6] have been observed in many different mixtures including granular systems by simple computer simulation models [7,8], e.g., pattern-forming segregation [9], lane formation [10], segregation and mixing [11–16]. Enormous efforts have been made in recent years to understand the structural evolutions in particulate mixtures by lattice gas [17,18], molecular dynamics [19,20], and Monte Carlo [21] methods. Distribution of dissimilar constituent particles leads to random yet well-defined structural patterns [22,16] as a function of parameters such as interaction and temperature.

Why the distribution of constituents, their specific mixtures, and underlying patterns in a steady-state flow of multi-component system are important? It is now well known among the geophysics, geology, oil and gas exploration and research community that the existence of methane hydrate below the ocean floor nearly throughout the continental shelf offers abundance of energy resources that exceed nearly all the natural and fossil fuel together [1,2]. The kinetics of hydrate formation [1], i.e., the chemistry and its thermodynamic stability is well understood experimentally and theoretically (computationally in particular). The origin of methane gas below the ocean floor also is reasonably well understood. Reduction of organic matter by bacteria (generally within tens of meters of the seafloor) generates what is referred to as biogenic methane; this is the most widely distributed form of methane in the marine environment. Leakage of methane from deep petroleum reserves through faults in the sediments places thermogenic methane near the seafloor especially in areas with significant petroleum reserves (e.g., the Gulf of Mexico). The methane gas is buoyant and flows upward through the permeable sediments towards the water. The methane is under hydrostatic pressure and at a temperature determined by the local geothermal gradient; when the free methane gas (and water) reach the appropriate pressure–temperature regime methane hydrate can form. The continuous supply of methane gas, formation of methane hydrate and its dissociation are on-going geothermal processes which lead to their steady-state distribution and instabilities with varying time and spatial scales. Of course, the enormous magnitude of scale, diversity of emerging phenomena (dissociation of methane gas to eruption of mud volcanoes below the ocean floor), and their implications and impacts are overwhelming to tackle in one computer simulation modeling. However, it is possible to examine patterns relevant in part of such complex system and learn the basic cause and effects of such parameters as the pressure bias and molecular

weight of constituents on their distribution via idealized computer simulation modeling.

In this article, we consider the flow of immiscible mixture of two components (A, B) of molecular weights M_A, M_B in an effective medium on a cubic lattice and examine the effects of molecular weight and pressure bias on the steady-state density distributions by an interacting lattice gas simulation. In particular, we address how the overall steady-state density of constituent particles and their profiles depend on the pressure bias and their molecular weights.

2. Model

We consider the mixture of two components A and B (each with molecular weight M_A and M_B) on a cubic lattice of size L^3 with $L = 30$–200. Particles A and B are randomly distributed initially at about 50% of the lattice sites with one particle at a site at any time. A nearest-neighbor interaction between particles (A, B) and empty (pore) sites (O) is described by

$$E = \sum_i \sum_n J(i,n)\,, \tag{1}$$

where index i runs over all sites occupied by particles and n over all nearest-neighbor sites of i. The interaction matrix elements

$$J(A,A) = J(B,B) = -J(A,B) = -J(B,A) = -\varepsilon\,, \tag{2a}$$

$$J(A,O) = J(B,O) = -1\,. \tag{2b}$$

The interaction strength $\varepsilon = 1$ describes the miscibility gap. The gravitational energy U of each particle with mass $M_{A/B}$ at the height z is given by

$$U = M_{A/B} z\,. \tag{3}$$

A source of particles is connected to the bottom plane ($z = 1$). This causes a concentration gradient (see below) which implicitly exerts a driving force upward. Additionally, we consider a pressure bias (H) caused by the hydrostatic pressure gradient to move constituent along vertical $(\pm z)$ direction with probabilities

$$H_{+z} = (1 + H)/6, \quad H_{-z} = (1 - H)/6, \quad 0 \leqslant H \leqslant 1\,. \tag{4}$$

Note that the hydrostatic pressure bias is implemented probabilistically (see below) and acts against sedimentation (Eq. (3)).

Each randomly selected particle (at site i) attempts to select a neighboring site (j) along $\pm x$ and $\pm y$ with equal probability $(\frac{1}{6})$ and along z (up) and $-z$ (down) directions with unequal probabilities (Eq. (4)) for non-zero hydrostatic bias H. The Metropolis algorithm is used to move randomly selected particles (A and B) to their neighboring empty sites with probability $\exp\{-(\Delta E + \Delta U)\}$. Note that the sedimentation probability is coupled with the gravitational potential energy (Eq. (3)) of constituents via Boltzmann distribution. When a particle at the bottom plane ($z = 1$) moves horizontally (xy-plane) or upward (to $z = 2$ plane), a new

particle (A or B) from the source is injected onto the vacated site according to their current lattice concentrations. Unlike our previous studies [15] where particles A and B enter the lattice with equal probability, the injection of particles depends on their concentrations (p_A, p_B) here. This introduces a concentration dependent interaction between the source and the system which lead to non-linear responses as we may see below. The cubic box is open along vertical boundaries, i.e., a particle can drop out when it attempts to move down from the bottom or escape from the top ($z = L$). Periodic boundary conditions are implemented along the transverse (x, y) directions. An attempt to move each particle once is defined as one Monte Carlo step (MCS) time. Almost all data presented here are generated on 100^3 sample. Different sample sizes are, however, used to check for the finite size effects. No severe finite size effect is observed on the qualitative behavior unless specified otherwise. The molecular weight ratio $\alpha = M_B/M_A$ is varied for a constant $M_A = 0.1$ and $\alpha = 1$–10.

The number and densities of particles and their distributions change as the simulation proceeds. Injection of particles from the source at the bottom leads to a net flow along the longitudinal direction. The competing driving fields due to hydrostatic pressure bias and gravity further affect the flow and pattern. A steady state is reached with a stable density profile and a constant rate of mass flux in asymptotic time limit. The simulation is repeated for a number of independent samples to obtain a reliable estimate of physical quantities. These quantities include, root mean square (rms) displacement of tracers (particles) and that of their center of mass, density profiles (longitudinal and transverse), correlation profiles (i.e., average number of different neighbors of each particles), flow rate and flux rate density, etc., as a function of bias H for different values of molecular weight ratios α. In this article, we constrain to structural response, i.e., changes in density profiles of A and B and their steady-state concentrations.

3. Results and discussion

Visualizations (on smaller samples) show how the two components re-arrange and segregate to a steady-state distribution as they continue to flow. Fig. 1 shows the snap-shots of their steady-state distributions for different bias (H) at the molecular weights $M_B = 0.8, 1.0$ for $M_A = 0.1$. Sedimentation and segregation are clearly seen at lower bias ($H = 0.2, 0.3$) and higher α. At low bias ($H = 0.2$), sedimentation dominates and the heavier constituents (B) settle down more toward the lower part of the lattice which has much higher density than the upper part with a dilute concentration of lighter constituents (A). Note that the distribution of particles remains the same while both constituents continue to flow from bottom to top. One may interpret the high density at the bottom, a representative of dissociating solid phase while the dilute region toward the top as a gas phase. Higher bias smears the phase separation by reducing the segregated gaseous domains of lower molecular weight component (A) by interspersing into the heavier component. Systems remain segregated with regions of partial layers and domains. The total density (number of

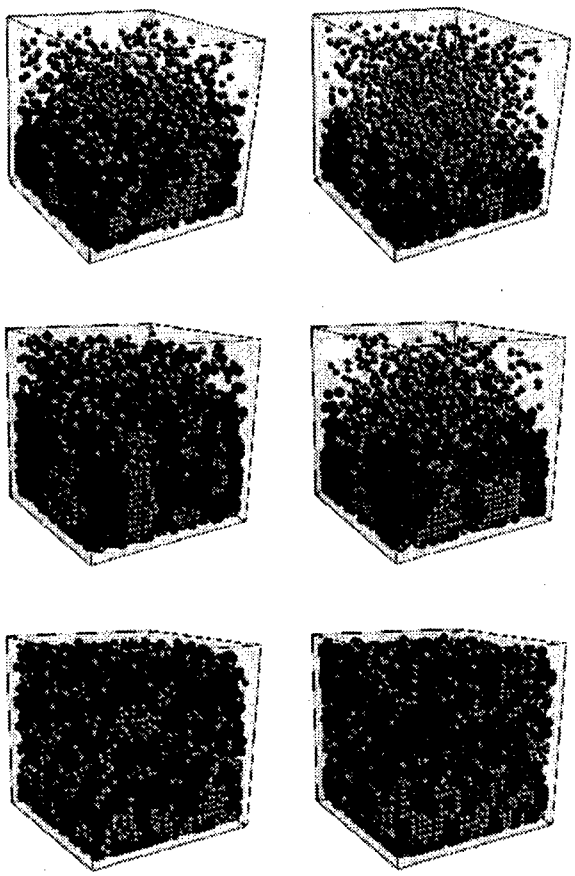

Fig. 1. Immiscible A (light, $M_A = 0.1$) and B (dark, $M_B = 0.8$ (left) 1.0 (right)) particles with pressure bias $E = 0.2, 0.3, 1.0$ at time steps $t = 2500$ with $\varepsilon = 1$. Injection of particles is proportional to their lattice concentration.

particles) in steady-state depends on the bias and molecular weight as will be seen below.

Fig. 2 shows a typical mass transfer (bottom to top) with time steps as a function of hydrostatic pressure bias ($H = 0.10$–1.0) for $\alpha = 8$. The flux rate (the slope of the mass transfer with time step) becomes constant which implies that our system has reached the steady state, i.e., the number of particles entering the system from the source is equal to their number leaving. Accordingly, the total number of particles in the sample remains constant with time step (see the inset figures). At low bias (i.e., $H \simeq 0.0$–0.3), the flux of heavier component (B) is lower than that of the lighter constituents (A). At high bias ($H \to 1$), the flux of B component becomes much larger than that of A resulting in a larger concentration of B in the lattice. This is due to concentration-dependent interaction between the source and the system-in-flux of

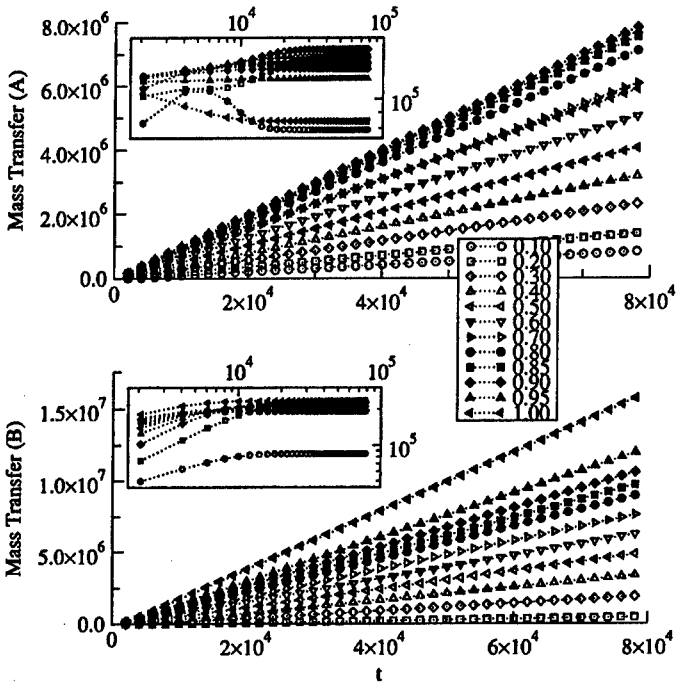

Fig. 2. Mass transfer versus time steps for various bias $H = 0.10$–1.00. Inset figures shows the number of corresponding particles in the simulation box. Sample size 100^3, $M_A = 0.1$, $M_B = 0.8$ with 128 independent runs.

particles B increases (in-flux of A decreases) according to their lattice concentration. The concentration-dependent in-flux from the source introduces a long-range (visco-elastic type) hydrodynamic interaction that may cause volcanic non-linear flow response, a topic of out future analysis.

As mentioned above the concentration gradient and the pressure bias are driving the constituents against gravitational sedimentation. In steady state, the density profiles remain constant in time while constituents continue to flow. Fig. 3 shows density profiles at bias $H = 0.1$ and 0.4 for different values of molecular weight ratios $\alpha = 1$–4. The longitudinal density profiles are very sensitive to α at low bias ($H = 0.1$) where gravity has profound effect leading to much larger densities of both constituents (A, B) towards the bottom. Still there is a net mass flow from bottom to top. The transverse (y) density profiles show oscillations, a signature of lane formation or partial longitudinal layering. Note that the complementary spatial oscillation in transverse density profiles of A and B constituents implies that they are segregated. Significant drop in the longitudinal density profile from bottom to top also shows a phase separation between high density at bottom (mostly B component) and low density A (gas) phases (see also Fig. 1). At higher bias ($H = 0.4$), such a visible layered segregation is reduced somewhat as the A constituents interspersed

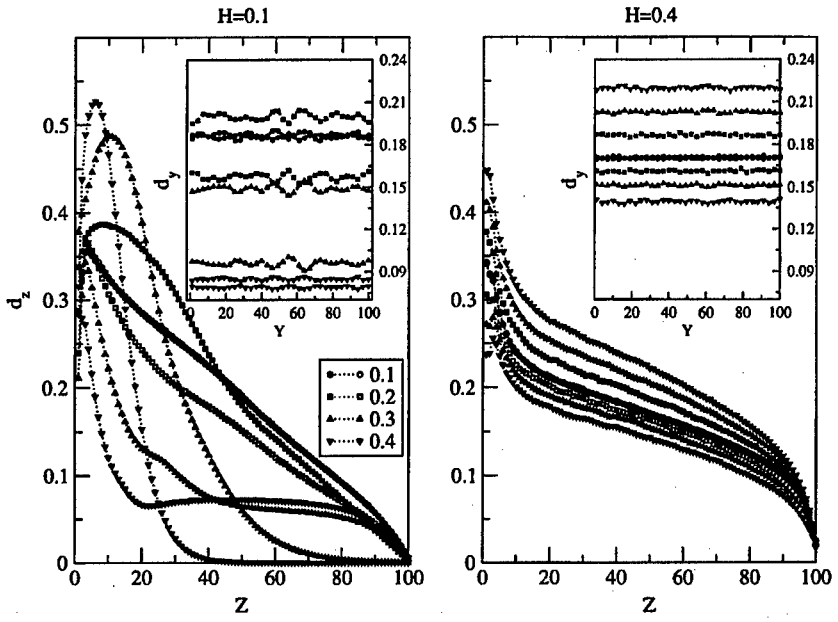

Fig. 3. Longitudinal and transverse (inset) density profiles at bias $H = 0.1$ and 0.4 for $M_A = 0.1$ and $M_B = 0.1$–0.4. Open symbols represents A and filled symbols B particles densities. Statistics is the same as Fig. 2.

into B. The linear decay region of the longitudinal density profile spans with a larger density of higher molecular weight component (see Fig. 3). Thus, the steady-state segregation of immiscible constituents (A, B) and phase separation of their high- and low-density phases along with a simultaneous flow show dissociating characteristics of complex evolutionary systems, i.e., the formation of methane hydrate and its dissociation below the ocean floor [1–4].

Such an open dynamic system in which the number of constituents are not conserved, exhibits stable density profiles and distinct phases with specific concentration distributions that depend on the hydrostatic pressure and molecular weight at a fixed temperature ($T = 1$ in unit of Boltzmann constant here). Obviously the total number of constituents (i.e., their overall densities) depends on pressure bias and α. Fig. 4 shows the dependence of the number of particles on the bias H for a range of molecular weight ratios, $\alpha = 1$–10. We immediately note a symmetry in the distributions of these constituents. At $\alpha = 1$, the distribution of A and B coincides at all bias with nearly a constant value of their concentrations. At higher values of α, the number of B constituents (higher molecular weight) become larger than that of A with a highly nonlinear rate of change at extreme values of $H \simeq 0.8$–1.0. The variation of the steady state (i.e., nearly constant) numbers of A and B with the bias becomes non-monotonic at high molecular weight ratio ($\alpha = 8, 10$). While the number of A particles shows a maximum, the number of B particles shows a minimum around $H \simeq 0.83$.

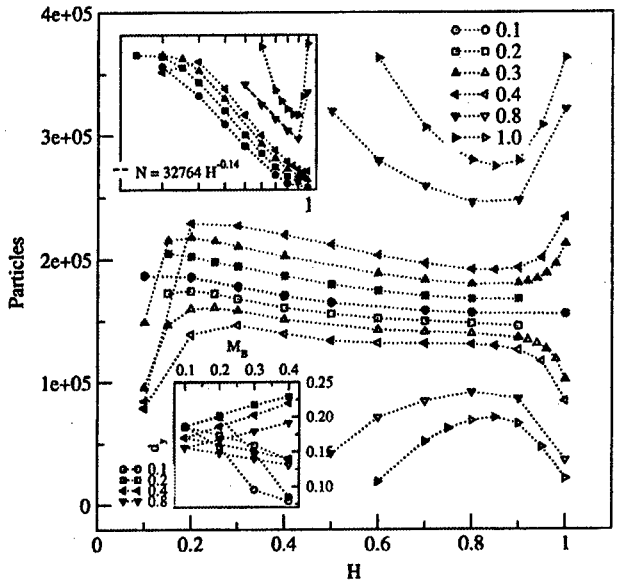

Fig. 4. Number of A, B, and their total numbers in steady-state versus bias H for $M_A = 0.1$ and $M_B = 0.1$–1.0 (upper legend). Top inset figure shows the total number of particles versus H on a log–log scale. Lower inset figure shows the variation of average transverse (y) density with M_B at $H = 0.1$–0.8 (lower left legend). Open symbols (A), filled symbols (B), statistics is the same as Fig. 2.

It is important to point out that, despite the higher molecular weight of B (higher sedimentation rate) in comparison to that of A, the number N_B of B particles becomes much larger than N_A at extreme values of $H \to 1$. We believe that this is due an implicit interaction between constituents and their source: the release of particles from the source into the system depends on their fraction in the lattice causing a flow-induced long-range hydrodynamic interaction among the heavier constituents. Both components (A, B) are driven upward by the bias with equal probability. However, B constituents have lower probability to leave the system from the top than that of A constituents on increasing the weight ratio α from 1, which results in a higher concentration and therefore higher injection of B. One may view the molecular weight (M_A, M_B) of particles as a 'sticky' long range overall (attractive elastic) interaction with the source which increases with their concentration. This results in a non-linear surge of heavier component and decay of lighter component accordingly as reflected in the flow response (to be discussed some where else).

Can we quantify the dependence of the total number (N) of these constituents as a function of hydrostatic pressure bias? In an attempt to address this question, we have examined the variation of N with the bias H. The inset figure (top) shows such a variation on a log–log scale which suggest a weak power-law decay $N \propto H^{-0.14}$ in the moderate range of H (see inset Fig. 4). The plot on a log-normal scale does not look much different. The empirical dependence may be more complex than just power-law

and exponential; perhaps it is a combination of both with the possibility of stretched exponential decay of N with the bias H which is difficult to identify with the current data. At large molecular weight ratio ($\alpha \geqslant 8$–10), the non-monotonic dependence of N on H seem to suggest that a non-linear structure with specified density can emerge in such a driven system. Large-scale examples may include berm formation in explosive detonation and in settling of lava flow after a volcanic response. From the transverse density profiles (see Fig. 3), one may evaluate the average density d_y. Variation of d_y with the molecular weight (M_B or α) for different bias (see the lower inset Fig. 4) suggests that d_y of A component decreases linearly while that of the B component increases with α for $H \geqslant 0.2$. At lower bias ($H \leqslant 0.1$), transverse densities of both components (A, B) decays as the sedimentation dominates.

4. Conclusions

In summary, structural responses of a multi-component driven system are studied by an interacting lattice gas model. Immiscible components (A, B) are driven from a source by concentration gradient and hydrostatic pressure bias against gravitational sedimentation in an effective medium. The hydrostatic pressure bias H and the molecular weight ratio are varied in this open system. A steady-state structural pattern emerges at a fixed bias and molecular weight with specific density profiles of each component as they continue their steady flow. In addition to phenomenological interactions among the constituents (Eqs. (1,2)), gravity, and pressure bias, an implicit hydrodynamic interaction develops as the injection of constituents in system depends on their lattice concentration. The number of each constituents reaches a stable value (nearly a constant) in steady state.

The longitudinal density profiles depend on bias and molecular weight with a range of patterns (non-linear, exponential, linear) for the dependence of density on the altitude. The transverse density profiles show segregation with partial layering for specific values of bias and molecular weight. Number of B constituents (higher molecular weight) are higher than that of A; the difference increases on increasing the molecular weight of B. The total number of particles shows a weak dependence on the bias, $N \propto H^{-0.14}$ for moderate range of bias ($0.2 \leqslant H \leqslant 0.8$) for $\alpha = 1$–8. At large molecular weight ratios ($\alpha \geqslant 8$), N becomes non-monotonic as a function of bias with a minimum (at about $H \geqslant 0.83$); the number of A and B constituents show complementary dependence, i.e., maximum and minimum, respectively, as function of bias. The large response of the overall density of heavier components at high bias ($H \to 1$) is a signature of volcanic response—a result of the flow—induced long-range hydrodynamic interaction with the source caused by the concentration dependent in-flux. Thus, specific density distributions with segregation and phase separation appear in an open system—pattern and phase boundaries can be predicted at least empirically as a function of hydrostatic bias and molecular weight. How realistic are these predictions remain to be seen as the large-scale geomarine exploration continue to probe the morphological evolution of methane hydrate and related components [1–3].

Acknowledgements

We acknowledge partial support from ONR PE # 0601153N and NSF-EPSCoR grants. This work was supported in part by grants of computer time from the DOD High Performance Computing Modernization Program at the Major Shared Resource Center (MSRC), NAVO, Stennis Space Center.

References

[1] E.D. Sloan, Clathrate Hydrates of Natural Gases, second ed., Marcel Dekker, New York, 1997.
[2] Proceedings of the Fourth International Conference on Gas Hydrate, Yokohama, 2002.
[3] W.T. Wood, J.F. Gettrust, in: C.K. Paul, W.P. Dillon (Eds.), Natural Gas Hydrates: Occurrence, Distribution, and Dynamics, AGU Monograph, vol. 124, 2001, p. 165.
[4] Chuang Ji, G. Ahmadi, W. Zhang, D.H. Smith, in: Proceedings of the Fourth International Conference on Gas Hydrate, Yokohama, 2002, p. 791.
[5] Hisashi O. Kono, B. Budhijanto, S. Narasimhan, D.H. Smith, in: Proceedings of the Fourth International Conference on Gas Hydrate, Yokohama, 2002, p. 543.
[6] H.A. Makse, S. Havlin, P.R. King, H.E. Stanley, in: L. Schimansky-Geier, T. Poeschel (Eds.), Novel Pattern Formation in Granular Matter, Springer, Heidelberg, 1997, p. 319.
[7] H.A. Makse, Physica A 330 (2003) 83.
[8] M. Latzel, S. Luding, H.J. Herrmann, Granular Matter 2 (2000) 123.
[9] T. Mullin, Phys. Rev. Lett. 84 (2000) 4741.
[10] J. Dzubiella, G.P. Hoffmann, H. Lowen, Phys. Rev. E 65 (2002) 021402.
[11] D.C. Rapaport, Phys. Rev. E 65 (2002) 61306.
[12] P. Biswas, P. Sanchez, M.R. Swift, P.J. King, Phys. Rev. E 68 (2003) 050301.
[13] E. Villermaux, J. Duplat, Phys. Rev. Lett. 91 (2003) 184501.
[14] A.C. Lund, C.A. Schuh, Phys. Rev. Lett. 91 (2003) 23505.
[15] R.B. Pandey, D. Stauffer, R. Seyfarth, Luis A. Cueva, J.F. Gettrust, Warren Wood, Physica A 310 (2002) 325.
[16] R.B. Pandey, J.F. Gettrust, R. Seyfarth, Luis A. Cueva, Int. J. Mod. Phys. C 14 (2003) 955.
[17] A. Xu, G. Gonnella, A. Lamura, Physica A 331 (2004) 10.
[18] L.O.E. Santos, P.C. Facin, P.C. Philippi, Phys. Rev. E 68 (2003) 056302.
[19] M.C. Mitchell, J.D. Autry, T.M. Nenoff, Molecular Phys. 99 (2001) 1831.
[20] G. Foffi, W. Gotze, F. Sciortino, P. Tartaglia, Th. Voigtmann, Phys. Rev. E 69 (2004) 011505.
[21] R. Finken, J.P. Hansen, A.A. Louis, J. Phys. A: Mathematical and General 37 (2004) 577.
[22] R. Consiglio, D.R. Baker, G. Paul, H.E. Stanley, Physica A 319 (2003) 49.